Adsorption 8: 291–299, 2002

Determination of a Solid Phase Mass Transfer Coefficient for Modeling an Adsorption Bed System Using Ammonium Molybdophosphate-Polyacrylonitrile (AMP-PAN) as a Sorbent for the Removal of ^{137}Cs from Acidic Nuclear Waste Solutions*

T.J. TRANTER†, R.S. HERBST AND T.A. TODD
BBWI, Inc., Idaho National Engineering and Environmental Laboratory, Idaho Falls, ID 83415, USA
ttranter@INEL.gov

Received October 19, 2001; Revised May 30, 2002; Accepted July 15, 2002

Abstract. Ammonium molybdophosphate (AMP) immobilized on a polyacrylonitrile (PAN) support is an engineered form of cesium selective sorbent material developed at the Czech Technical University in Prague. This material is being investigated as a sorbent for removing ^{137}Cs from Idaho National Engineering and Environmental Laboratory (INEEL) acidic sodium bearing waste (SBW) solution. As part of this study, a computer program to solve the partial differential equations (PDE's) for continuity and rate of exchange in a fixed bed system has been developed using numerical finite difference algorithms. These equations are solved iteratively in order to derive a mass transfer coefficient that agrees with the results of bench scale column experiments. This mass transfer coefficient is then applied in the PDE solutions to predict breakthrough behavior in a semi-scale column experiment. The model provided excellent agreement with the semi-scale data with a mass transfer coefficient of 0.0126 min^{-1}.

Keywords: ammonium molybdophosphate, polyacrylonitrile, cesium-137, nuclear waste, adsorption, fixed bed

1. Introduction

1.1. Historical Background

The Idaho Nuclear Engineering and Technology Center (INTEC), formerly known as the Idaho Chemical Processing Plant (ICPP), is located at the Idaho National Engineering and Environmental Laboratory (INEEL) near of Idaho Falls, Idaho. The main purpose of this Department of Energy (DOE) facility was the reprocessing of spent nuclear fuel from U.S. Navy and government owned nuclear reactors using a combination PUREX/REDOX process. The primary waste stream from this process was an acidic and highly radioactive raffinate stream containing fission, transuranic, and activation isotopes. The majority of this waste was calcined in a fluidized bed at 500°C to form a granular solid oxide. However, in addition to calcine waste, liquid sodium-bearing waste (SBW) was also generated as a result of combining solvent scrub and mineral acid decontamination solutions. This waste solution contains molar concentrations of sodium as well as moderate activity concentrations of transuranic and fission product isotopes. Currently, over 5 million liters of this liquid waste are stored in underground, concrete enclosed stainless steel tanks at the Idaho Nuclear Technology and Engineering Center (INTEC). The INEEL has investigated numerous separation options for removing the actinide and high activity fission isotopes from the SBW prior to final disposition. As part of that effort, the composite sorbent ammonium molybdophosphate polyacrilonitrile (AMP-PAN) was evaluated as an exchanger for cesium removal. The merits of this AMP-PAN sorbent, as well as bench scale experiments to

*Work performed for the U.S. Department of Energy under Contract No. DE-AC07-94ID13223.
†To whom correspondence should be addressed.

derive isotherms and breakthrough curves, were presented in detail in a previous paper (Tranter et al., 2002). The results of those tests showed that kinetics were predominately particle diffusion controlled. The purpose of the work described herein is to numerically solve the differential transport equations for continuity and rate of exchange for the AMP-PAN system in order to elucidate a mass transfer coefficient for diffusion in the solid particle phase.

2. Experimental/Methodology

AMP-PAN is a composite sorbent material consisting of approximately 85 wt% AMP in a porous PAN support. This material was developed by Sebesta et al. (1996) to provide an engineered form of AMP sorbent to be used in a packed bed. As described in previous work (Tranter et al., 2002), a series of bench scale experiments were performed with 1.5 cm^3 beds of AMP-PAN to obtain breakthrough data with a simulated sodium bearing waste (SBW) solution. A semi-scale test was then performed by Herbst et al. (2000) in which two 60 cm^3 AMP-PAN beds were tested as part of an integrated flowsheet with solvent extraction processes for actinide and strontium removal. Simulated SBW was used for this semi-scale test and the AMP-PAN columns were operated in series at the head-end of the separation flowsheet to remove cesium. The objective of the work presented in this paper is to use the data from the 1.5 cm^3 column tests to derive a mass transfer coefficient (k_pa) for the SBW/AMP-PAN system. This mass transfer coefficient is then used to predict the breakthrough curve for the 60 cm^3 columns in the semi-scale run. To this end, the fundamental transport equations are solved numerically using the small column data. This is done iteratively with different values of k_pa until an acceptable agreement with the experimental data is obtained. To simplify the calculations, the dispersion term in the continuity equation is neglected and k_pa is assumed to be constant for the SBW/AMP-PAN system. The system is also treated as single component adsorption or ion exchange. This is assumed to be valid since it has been shown (Smit, 1990) that AMP is highly selective for Cs and exhibits a selectivity sequence for the alkali metals similar to other heteropolyacids of the Keggin structure; $Cs^+ > Rb^+ > K^+ > Na^+ > Li^+$.

The composition of the simulated SBW feed solution is shown in Table 1. The experimental equipment and conditions for the column tests are described in detail in the previous reports by Tranter et al. (2002) and Herbst et al. (2000) and will not be repeated here. However, the experimental breakthrough data from the 1.5 cm^3 and 60 cm^3tests are shown in Figs. 1 through 3.

Table 1. Simulated SBW feed concentrations.

Component	Units	SBW simulant for 1.5 cm^3 tests	SBW simulant for 60 cm^3 integrated test
H^+	moles/L	1.31	1.55
Al	moles/L	5.9E-01	5.4E-01
B	moles/L	1.5E-02	1.8E-02
Ca	moles/L	3.3E-02	4.5E-02
Cl	moles/L	3.4E-02	4.1E-03
Cr	moles/L	6.0E-03	5.0E-03
Cs	moles/L	6.79E-05	1.0E-03
F	moles/L	No analysis	2.59E-01
Fe	moles/L	2.4E-02	2.03E-02
Hg	moles/L	1.8E-03	2.0E-03
K	moles/L	1.3E-01	1.18E-01
Na	moles/L	1.04	1.24
NO_3^-	moles/L	4.2	No analysis
SO_4^{-2}	moles/L	8.85E-03	No analysis
Pb	moles/L	9.56E-04	1.0E-03
Sr	moles/L	5.57E-03	1.0E-03
Zr	moles/L	5.78E-04	1.4E-03

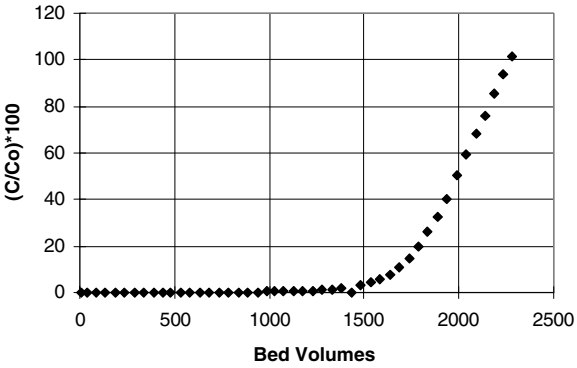

Figure 1. Cs breakthrough curve with simulated SBW. Flow rate = 25.3 BV/h, bed volume = 1.5 mL.

2.1. *Equilibrium Isotherm*

Equilibrium isotherm data for the simulated SBW—AMP-PAN system have been reported (Tranter et al., 2002). However, these experiments obtained limited data at the concentration range of interest for the present

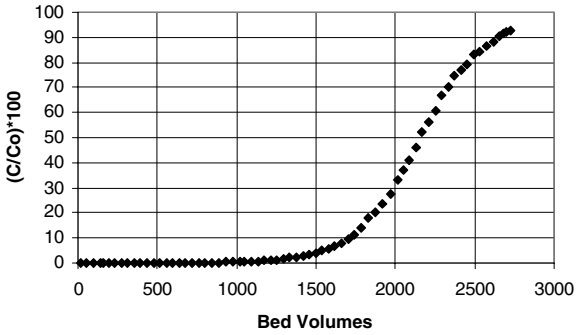

Figure 2. Cs breakthrough curve with simulated SBW. Flow rate = 39 BV/h, bed volume = 1.5 mL.

study. Therefore, additional equilibrium batch contacts were performed to obtain more data points at the lower end of the isotherm. Simulated SBW was spiked with a known amount of ^{137}Cs and stable ^{133}Cs. The feed solutions were then contacted with quantitative amounts of AMP-PAN for 48 hours at $23 \pm 2^{\circ}$C, according to the method previously described (Tranter et al., 2002). Aliquots of the aqueous solution were filtered and analyzed by gamma spectrometry using a high purity germanium (HPGe) detector coupled to a SUN® workstation. Equilibrium cesium concentrations in the aqueous fraction were determined by ratio of the radioactive ^{137}Cs to total cesium. Cesium concentrations in the solid phase were calculated by material balance.

2.2. *Column Modeling*

Developing a model to accurately describe adsorption or ion exchange in a fixed bed system is inherently difficult. Since the concentration of the adsorbate or counter-ion changes as the feed moves through the bed, the process does not operate at steady state. Design equations derived to model the system with theoretical rigor are differential in nature and usually require complex numerical methods to solve. Some solutions for very limiting cases have been reported (Cooper, 1965, 1970; Thomas, 1948; Vermeulen, 1953) but, in general, complete time-dependent analytical solutions to differential equation based models of the proposed rate mechanisms are not available. The fundamental transport equations for a fixed bed are the solid-fluid material balance and rate of exchange. If dispersion is neglected, these equations can be written in the following form (Klein, 1983):

$$\frac{\partial c}{\partial t} + v\frac{\partial c}{\partial z} + \frac{(1-\varepsilon)}{\varepsilon}\frac{\partial q}{\partial t} = 0 \quad \textit{material balance} \quad (1)$$

$$\frac{\partial q}{\partial t} = k_p a F(c, q) \quad \textit{solute exchange rate} \quad (2)$$

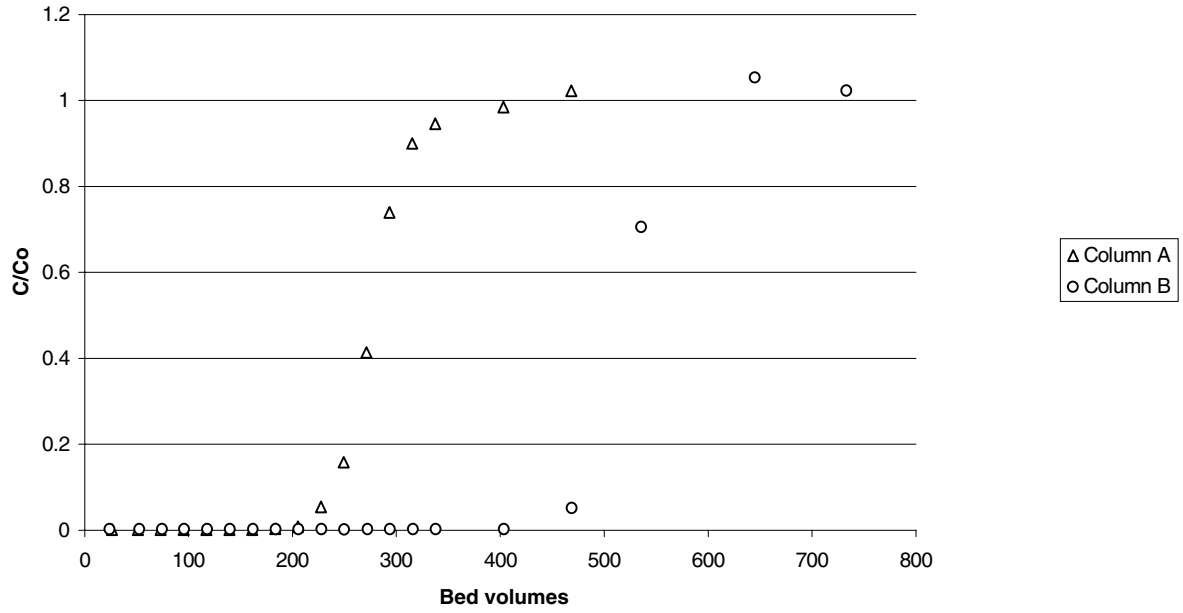

Figure 3. Cs breakthrough curves with simulated SBW waste, semi-scale columns A and B. Flow rate = 22 BV/h, BV column A = BV column B = 60 mL.

Where:

$\varepsilon =$ the void fraction or fluid filled spaces between particles, 0.78
$v =$ the average interstitial fluid velocity between the particles, cm/min
$z =$ the distance from the bed inlet in the axial direction, cm
$c, q =$ the fluid and solid phase concentrations, respectively, mol/cm^3
$k_p a =$ the interphase mass transfer coefficient, min^{-1}
$F(c, q) =$ a driving force to be specified
$t =$ time, min.

Since it was shown by Tranter et al. (2002) that the AMP-PAN system is primarily limited by diffusion in the particle phase, a linear driving force in terms of the solid phase concentration was chosen to represent $F(c, q)$. Therefore, Eq. (2) can be re-written as:

$$\frac{\partial q}{\partial t} = k_p a(q^* - q) \quad \textit{solute exchange rate} \qquad (3)$$

Where:

$q^* =$ the solid phase concentration in equilibrium with the concentration in the liquid (c) at time t, mol/cm^3.

It then follows that an equilibrium relationship between the solid and liquid phase must be specified. For this analysis, the Langmuir equation was used for the equilibrium equation and is of the form:

$$q^* = \frac{KcQ_0}{1 + Kc} \qquad (4)$$

Where:

$K =$ equilibrium constant for the exchange of Cs in AMP, cm^3/mol
$Q_0 =$ the asymptotic maximum solid phase concentration, mol/cm^3.

The data obtained from the equilibrium batch contacts, as described previously in Section 2.1, yield a classical Type I isotherm. Consequently, they were fit reasonably well with the Langmuir model ($R^2 = 0.956$) and are presented in Fig. 4. The Langmuir coefficients derived from this fit are used in the model to calculate equilibrium values for the solid phase, q^*. These coefficients are listed in Table 2.

Inspection of Eqs. (1) and (2) reveals that they are a system of linear, parabolic, partial differential equations (PDE) of the first order. The method of finite differences is used to obtain the numerical solution of these transport equations. However, before expanding these equations in finite difference form, it is more convenient to reformulate the independent variables in terms of dimensionless variables:

$$x = \frac{z}{L}; \quad \tau = \frac{L}{v}; \quad \theta = \frac{t}{\tau} \qquad (5)$$

Where:

$x =$ dimensionless length
$\tau =$ residence time in the bed, min
$\theta =$ dimensionless time of operation
$L =$ total bed height, cm

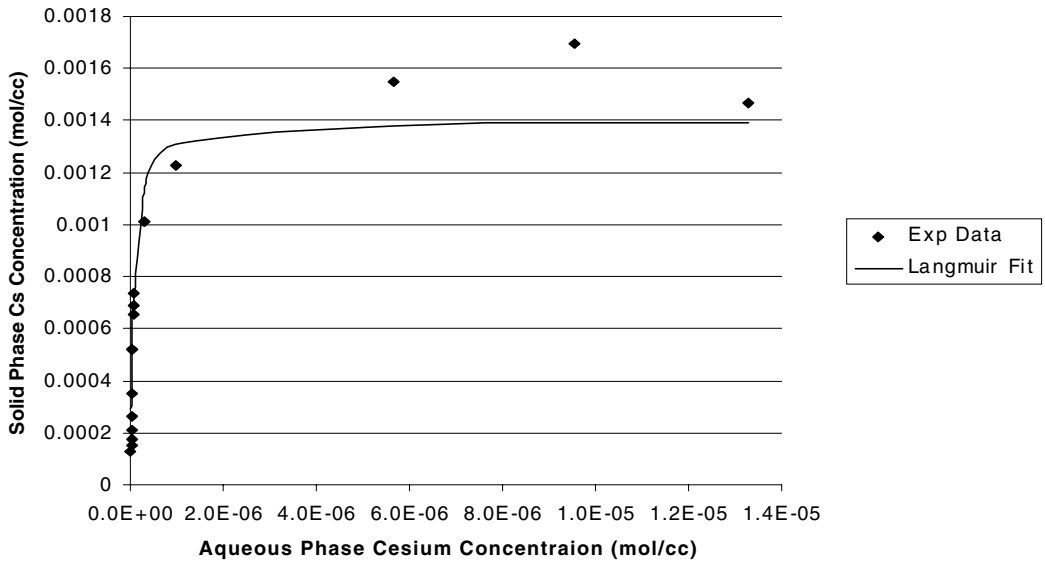

Figure 4. Equilibrium isotherm for simulated SBW—AMP-PAN system at 23 ± 2°C.

Table 2. Langmiur coefficients, AMP-PAN bulk, and absolute density.

Test	Langmuir equilibrium constant K	Q_0 asymptotic max concentration, mole/cm^3 of AMP-PAN	Bulk density of AMP-PAN (g/cm^3)	Absolute solid particle density of AMP-PAN (g/cm^3)
25.3 BV/h 1.5 cc column	1.5E+07	0.001398	0.61	2.797
38.7 BV/h 1.5 cc column	1.5E+07	0.001398	0.61	2.797
21.7 BV/h 60 cc semi-scale column A	1.5E+07	0.001398	0.61	2.797
21.7 BV/h 60 cc semi-scale column B	1.5E+07	0.001398	0.61	2.797

Then:

$$\frac{\partial t}{\partial \theta} = \tau \quad \text{and} \quad \frac{\partial \mathrm{z}}{\partial x} = \tau v = L \tag{6}$$

and

$$\begin{aligned} \frac{\partial c}{\partial t} &= \frac{1}{\tau}\frac{\partial c}{\partial \theta} \\ \frac{\partial c}{\partial z} &= \frac{1}{\tau v}\frac{\partial c}{\partial x} \\ \frac{\partial q}{\partial t} &= \frac{1}{\tau}\frac{\partial q}{\partial \theta} \end{aligned} \tag{7}$$

When the above relationships are substituted into Eq. (1), the τ, v, ∂t, and ∂z terms cancel leaving the equation in the form:

$$\frac{\partial c}{\partial \theta} + \frac{\partial c}{\partial x} + \left(\frac{1-\varepsilon}{\varepsilon}\right)\frac{\partial q}{\partial \theta} = 0 \tag{8}$$

Applying the same derivation to Eq. (3) transforms it into the form:

$$\frac{\partial q}{\partial \theta} = \tau k_p a \left(q^* - q\right) \tag{9}$$

The differential terms in Eq. (8) can now be expanded into finite difference form:

$$\left(\frac{c_i^{l+1} - c_i^l}{\Delta\theta}\right) + \left(\frac{c_i^l - c_{i-1}^l}{\Delta x}\right) + \frac{1-\varepsilon}{\varepsilon}\left(\frac{q_i^{l+1} - q_i^l}{\Delta\theta}\right) = 0 \tag{10}$$

In the above equation, the temporal derivatives are written as forward differences while the spatial derivative is written as a backward difference. The scripts i and l refer to the space and time steps, respectively. Since the objective is to calculate the concentration profile axially through the column, Eq. (10) is written to solve explicitly for the $l+1$ time step at each spatial point:

$$c_i^{l+1} = c_i^l + \frac{\Delta\theta}{\Delta x}\left(c_{i-1}^l - c_i^l\right) - \frac{1-\varepsilon}{\varepsilon}\left(q_i^{l+1} - q_i^l\right) \tag{11}$$

Following a similar derivation, the equation for solute exchange rate is written as a forward difference:

$$q_i^{l+1} = q_i^l + \Delta\theta\tau k_p a\left(q_i^{l^*} - q_i^l\right) \tag{12}$$

The initial (I.C.) and boundary (B.C.) conditions are specified as follows:

$$\begin{aligned} &\text{I.C.} \quad c = q = 0\,(x, 0) \\ &\text{B.C.} \quad c = c_0\,(0, t) \\ &\qquad \frac{\partial c}{\partial x} = 0\,(x = L, t) \end{aligned} \tag{13}$$

The finite difference relationships in Eqs. (11) and (12) were coded into visual basic along with the I.C. and B.C. parameters. The grid was chosen to solve for the liquid and solid phase concentrations, c and q, at 20 evenly spaced axial points through the column. This in turn specified the time step since the $\triangle\theta/\triangle x$ term was set at $\leq$0.5 to obtain a stable solution. A value for the mass transfer coefficient, $k_p a$, was specified and the program executed. The run time for the program was approximately 5 minutes using a 1 GHz processor. During program execution, a plot of the calculated breakthrough curve was generated in "overlay" fashion in the same coordinates as the 1.5 cm^3 experimental data. In this way, the slope of the calculated curve could be visually compared to the experimental data and the next value of $k_p a$ chosen to increase or decrease the slope as necessary. This process was repeated iteratively until the slope of the calculated curve and the

calculated effluent liquid concentration at 50% breakthrough were nearly coincident with the experimental data. The final value for $k_p a$ was then used in the numerical program, along with the appropriate values for column size and fluid velocity, to generate a predicted breakthrough curve for the 60 cm^3 column run.

3. Results and Discussion

The PDE solution program was executed approximately 8 times in order to converge on the best value of $k_p a$. The value obtained for the SBW/AMP-PAN system was $k_p a = 0.0126\ min^{-1}$. A plot showing the calculated breakthrough curve and the experimental data for the 1.5 cm^3, 25.3 bed volume per hour (BV/h) test and the 1.5 cm^3, 38.7 BV/h test is shown in Fig. 5. It can be seen that the $k_p a$ value of $0.0126\ min^{-1}$ resulted in excellent agreement with the 25.3 BV/h experimental data from the 1.5 cm^3 column test with a determination coefficient (R^2) of 0.996. Agreement with the 38.7 BV/h test in the 1.5 cm^3 column was not quite as good but still very acceptable with $R^2 = 0.981$.

Plots of the predicted curves (with $k_p a = 0.0126\ min^{-1}$) for the 60 cm^3 semi-scale test columns IX A and B, along with the corresponding experimental data, are presented in Figs. 6 and 7. To generate the curve for the second column (IX B) in the series, the system was modeled as one 120 cm^3 column with the BV/h rate halved. It can be seen that the mass transfer coefficient derived from the small bench scale column data did an excellent job of predicting the breakthrough behavior of the 60 cm^3 tandem semi-scale column system, resulting in R^2 values of 0.984 and 0.943 for the IXA and IXB columns, respectively. This was true even when the column was modeled as one continuous system with twice the residence time. Also, as shown in Table 1, the Cs feed concentration in the semi-scale test was a factor of 15 higher than in the bench scale tests.

Numerically calculated liquid Cs concentration profiles for semi-scale column A as a function of time and axial distance through the column are shown in Fig. 8. It has been shown by Michaels (1952), that the length of the sorption zone, z_s, is a function of the column height, z, and the throughput volumes, V_B and V_T:

$$z_s = z\left[\frac{V_z}{V_T - 0.5V_z}\right] \tag{14}$$

Where:

V_B = volume processed at beginning of column breakthrough, BV
V_T = total volume processed at column exhaustion, BV
$V_z = V_T - V_B$

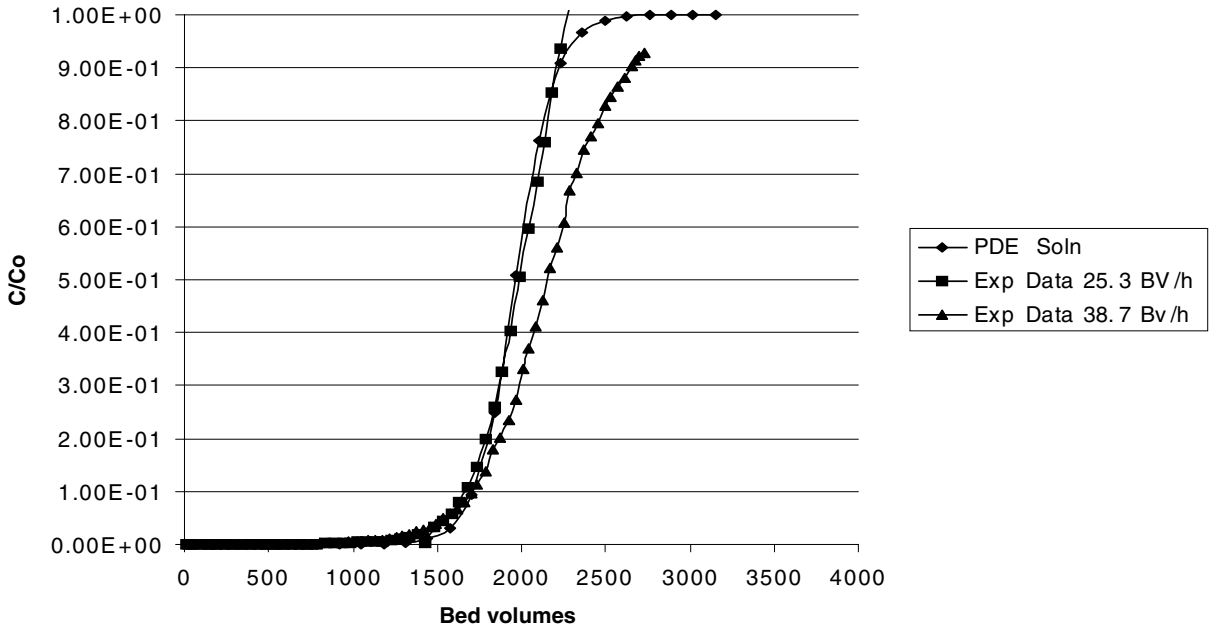

Figure 5. Experimental and predicted breakthrough curves for bench-scale test, bed volume = 1.5 mL, flow rate = 25.3 BV/h, $k_p a = 0.0126\ min^{-1}$.

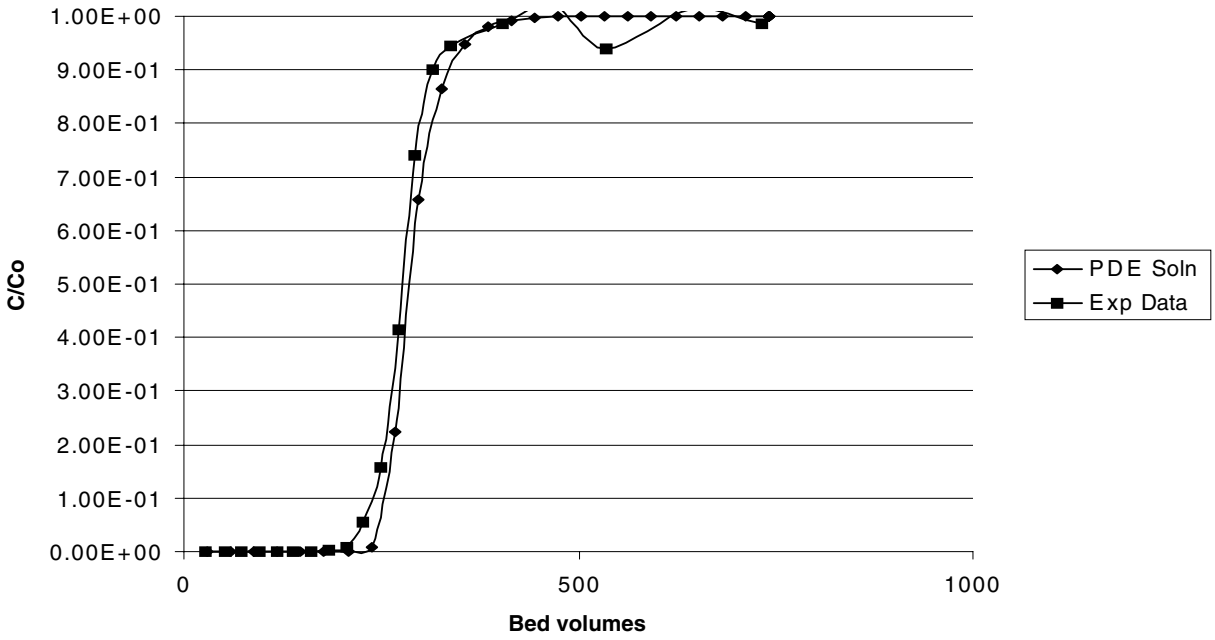

Figure 6. Experimental and predicted breakthrough curves for semi-scale test column A, bed volume = 60 mL, $k_p a = 0.0126\ \text{min}^{-1}$.

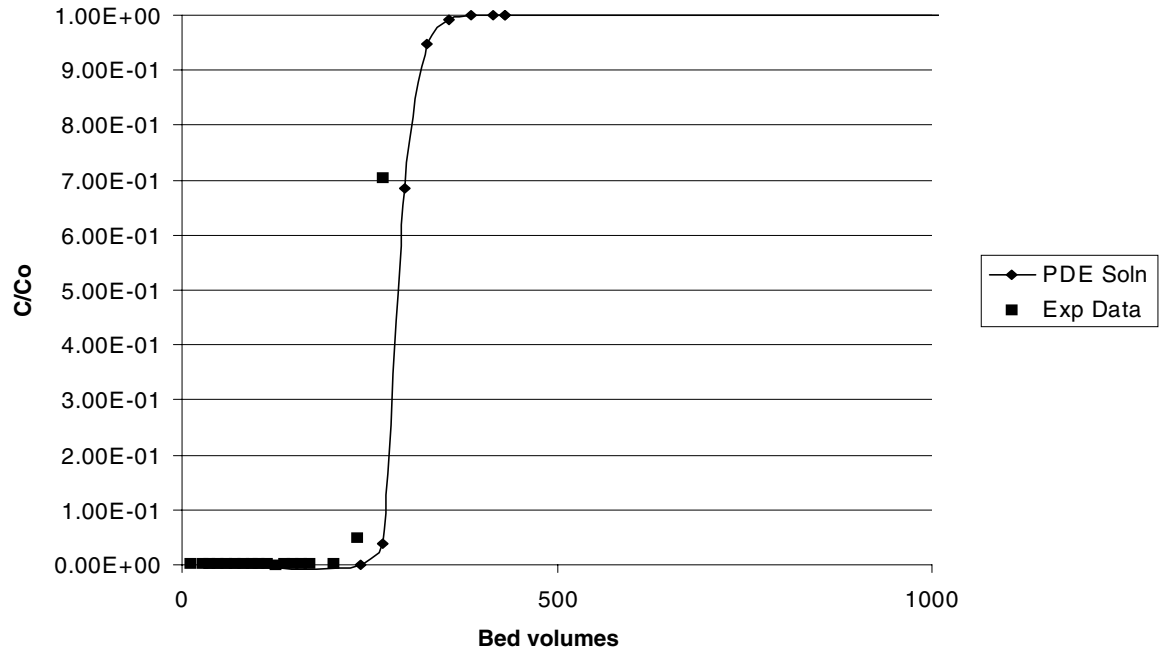

Figure 7. Experimental and predicted breakthrough curves for semi-scale test column B, bed volume = 60 mL, $k_p a = 0.0126\ \text{min}^{-1}$.

Using the values $V_T = 390$ BV, $V_B = 200$ BV and $z = 12$ cm obtained from the semi-scale column A experimental breakthrough data (Fig. 3), the solution to Eq. (14) indicates the length of the sorption zone to be approximately 7.5 cm. Inspection of the calculated concentration profiles in Fig. 8 also reveals the length of the sorption zone to be approximately 6–8 cm, which is in reasonable agreement.

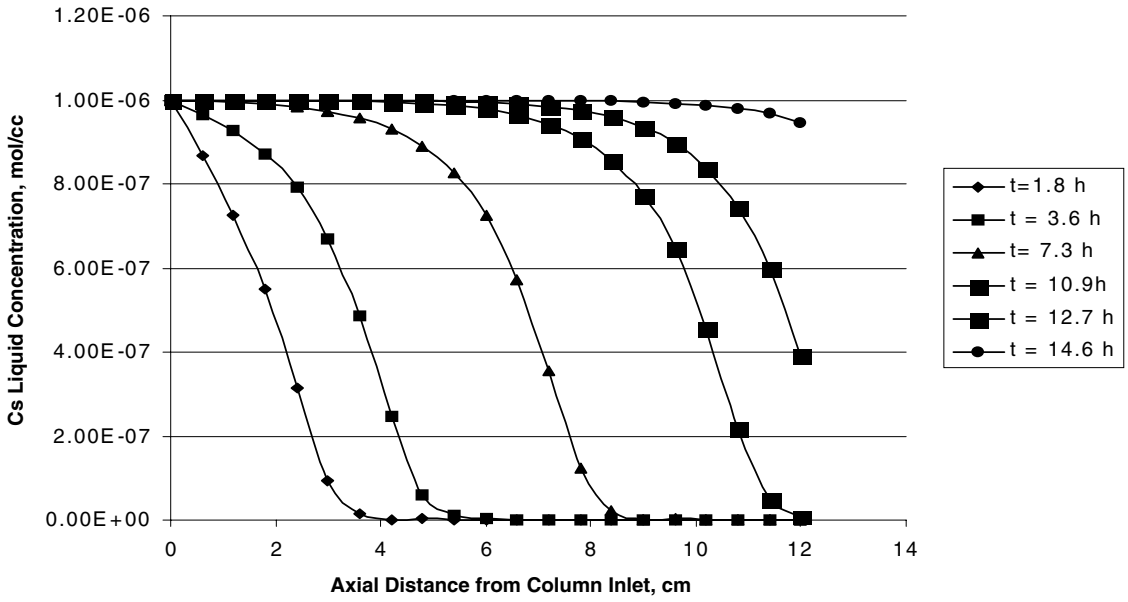

Figure 8. Calculated Liquid Cs concentration-time profiles for semi-scale column A. BV = 60 mL, $Z = 12$ cm, flow rate = 21.7 BV/h, 1.3 L/h.

4. Conclusions

The transport equations for continuity and rate of exchange have been numerically solved using data from small bench scale (1.5 cm^3) column experiments. The program to perform these calculations was developed using finite difference approximations for the differential terms in the PDE's. This approach yielded good results and eliminates the need for complex matrix algorithms which are required for finite element analysis. From these solutions, a mass transfer coefficient of 0.0126 min^{-1} for the SBW/AMP-PAN system was derived. This value for the mass transfer coefficient was used to successfully predict breakthrough behavior for an AMP-PAN semi-scale column system 80 times larger, with different flow rate, and a SBW Cs feed concentration 15 times higher. Therefore, the derived value for mass transfer coefficient used with the numerical solutions to the PDE's should be adequate for scale-up and estimating AMP-PAN column performance in pilot scale systems for treating SBW at the INEEL.

Nomenclature

ε	the void fraction or fluid filled spaces between particles
ρ_B	the bulk density of the solid phase (g/cm^3) (bulk volume)
ρ_a	the absolute density of the particles in the solid phase (g/cm^3)
v	the average interstitial fluid velocity between the particles (cm/min)
z	the distance from the bed inlet in the axial direction (cm)
c, q	the fluid and solid phase concentrations, respectively (mol/cc)
$k_p a$	the interphase mass transfer coefficient (min^{-1})
$F(c, q)$	a rate driving force to be specified
q^*	solid phase concentration in equilibrium with the concentration in the liquid (c) at time t (mol/cc)
K	equilibrium constant for the exchange of Cs in AMP
Q_0	the asymptotic maximum solid phase concentration (mol/cc)
L	length of the bed (cm)
x	dimensionless length
τ	residence time in the bed (min)
θ	dimensionless time of operation
$i-1, i, i+1$	subscripts denoting previous, current, and next distance steps in the numerical solution, progressing axially from column inlet to outlet.
$l-1, l, l+1$	superscripts denoting past, present, and future time steps in the numerically solution.

V_B volume processed at beginning of column breakthrough (BV)
V_T total volume processed at column exhaustion (BV)
V_z $V_T - V_B$
BV bed volumes or column volumes

Acknowledgments

The authors wish to acknowledge and thank those who aided in the completion of this project. These include Doug Thompson and Stacey Hill for providing excellent analytical and experimental support and Dr. Ferdinand Sebesta for providing the AMP-PAN sorbent material.

References

Cooper, R.S. and D.A. Liberman, "Slow Particle Diffusion in Ion Exchange Columns," *Ind. Eng. Chem. Fundam.*, **4**, 308 (1965).

Cooper, R.S. and D.A. Liberman, "Fixed Bed Adsorption Kinetics with Pore Diffusion Control," *Ind. Eng. Chem. Fundam.*, **9**, 620 (1970).

Helfferich, F., *Ion Exchange*, pp. 475–476, McGraw-Hill, New York, 1962.

Herbst, R.S., J.D. Law, T.A. Todd, D.J. Wood, T.G. Garn, and E.L. Wade, "Integrated AMP-PAN, TRUEX, and SREX Flowsheet Test to Remove Cesium, Surrogate Actinide Elements, and Strontium from INEEL Tank Waste Using Sorbent Columns and Centrifugal Contactors," Bechtel BWXT Idaho, INEEL/EXT-2000-00001, January 2000.

Klein, G., "Column Design for Sorption Processes," in *Mass Transfer and Kinetics of Ion Exchange,*L. Liberti and F.G. Helfferich (Eds.), pp. 226–227, Martinus Nijhoff, Boston, 1982.

Michaels, A.S., "Simplified Method of Interpreting Kinetics Data in Fixed-Bed Ion Exchange," *Ind. And Eng. Chem.*, **44**, 1920–1930 (1952).

Sebesta, F., J. John, and A. Motl, "Development of Composite Ion-exchangers and their use in Treatment of Liquid Radioactive Wastes," Czech Technical University of Prague, July 1996.

Smit, J. and R. van, "Insoluble Heteropolyacid Salts," in *Inorganic Ion Exhangers in Chemical Analysis*, M. Qureshi and K.G. Varshney (Eds.), pp. 68–69, CRC Press, Boston, 1991.

Thomas, H.C., "A Problem in Kinetics," *Anals of the New York Academy of Science,* **49**, 161 (1948).

Tranter, T.J., R.S. Herbst, T.A. Todd, A.L. Olson, and H.B. Eldredge, "Evaluation of Ammonium molybdophosphate-Polyacrylonitrile (AMP-PAN) as a Cesium Selective Sorbent for the Removal of Cs-137 from Acidic Nuclear Waste Streams," *Advances in Environmental Research*, **6**, 107–121 (2002).

Vermeulen, T., "Theory of Irreversible and Constant-Pattern Solid Diffusion," *Ind. Eng. Chem.*, **45**, 1664 (1953).